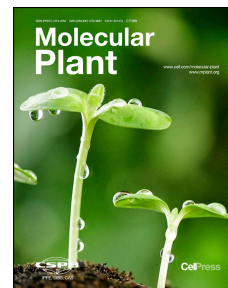# Accepted Manuscript

SUMOylation inhibition mediated by disruption of SUMO E1-E2 interactions confers plant susceptibility to necrotrophic fungal pathogens

Laura Castaño-Miquel, Abraham Mas, Inês Teixeira, Josep Seguí, Anna Perearnau, Bhagyasree N. Thampi, Arnaldo L. Schapire, Natalia Rodrigo, Gaelle La Verde, Silvia Manrique, Maria Coca, L. Maria Lois

Please cite this article as: **Castaño-Miquel L., Mas A., Teixeira I., Seguí J., Perearnau A., Thampi B.N., Schapire A.L., Rodrigo N., La Verde G., Manrique S., Coca M., and Lois L.M.** (2017). SUMOylation inhibition mediated by disruption of SUMO E1-E2 interactions confers plant susceptibility to necrotrophic fungal pathogens. Mol. Plant. doi: 10.1016/j.molp.2017.01.007.

This is a PDF file of an unedited manuscript that has been accepted for publication. As a service to our customers we are providing this early version of the manuscript. The manuscript will undergo copyediting, typesetting, and review of the resulting proof before it is published in its final form. Please note that during the production process errors may be discovered which could affect the content, and all legal disclaimers that apply to the journal pertain.

1 **<u>SUMOylation inhibition mediated by disruption of SUMO E1-E2 interactions</u>**

2 **<u>confers plant susceptibility to necrotrophic fungal pathogens</u>**.

3

4 Laura Castaño-Miquel, Abraham Mas, Inês Teixeira, Josep Seguí, Anna Perearnau,

5 Bhagyasree N. Thampi, Arnaldo L. Schapire, Natalia Rodrigo, Gaelle La Verde, Silvia

6 Manrique, Maria Coca, and L. Maria Lois[§].

7

8 Center for Research in Agricultural Genomics-CRAG.

9 Edifici CRAG-Campus UAB, Bellaterra (Cerdanyola del Vallés), 08193 Barcelona, Spain.

10

11 § Author for correspondence

12 L.Maria Lois

13 Center for Research in Agricultural Genomics-CRAG

14 Edifici CRAG-Campus UAB, Bellaterra (Cerdanyola del Vallés), 08193 Barcelona, Spain

15 Tel. +34 93 5636600 ext.3215

16 Fax. +34 93 5636601

17 email: maria.lois@cragenomica.es

18

19

20 **Running title**

21 SUMOylation impairment in necrotrophic attack

22

26

27 **Short Summary:**

28 Attachment of SUMO to proteins is an essential molecular mechanism that regulates plant

29 development and responses to environmental stresses. Based on structure-activity relationship, we

30 developed a strategy for inhibiting *in vivo* SUMO conjugation, and validated it by uncovering a novel

31 role of SUMO in defense responses to necrotrophic fungi, which constitutes a novel regulatory layer of

32 plant-fungus interactions.

33

34

1

35 **ABSTRACT**

36 Protein modification by SUMO modulates essential biological processes in eukaryotes.
37 SUMOylation is facilitated by the sequential action of the E1-activating, the E2-conjugating
38 and the E3-ligase enzymes. In plants, SUMO regulates plant development and stress
39 responses, which are key determinants in agricultural productivity. In order to generate
40 additional tools for advancing our knowledge of the SUMO biology, we have developed a
41 strategy for inhibiting *in vivo* SUMO conjugation based on disruption of SUMO E1-E2
42 interactions, by means of E1 SAE2^{UFDCt} domain expression. Targeted mutagenesis and
43 phylogenetic analyses revealed that this inhibition involves a short motif in SAE2^{UFDCt} highly
44 divergent across kingdoms. Transgenic plants expressing the SAE2^{UFDCt} domain displayed
45 dose-dependent SUMO conjugation inhibition, and have revealed the existence of a post-
46 transcriptional mechanism that regulates SUMO-E2 conjugating enzyme levels. In addition,
47 these plants displayed increased susceptibility to necrotrophic fungal infections by *Botrytis*
48 *cinerea* and *Plectosphaerella cucumerina*. Early after fungal inoculation, host SUMO
49 conjugation was post-transcriptionally down-regulated, suggesting that targeting
50 SUMOylation machinery could constitute a novel mechanism for fungal pathogenicity. These
51 findings support the role of SUMOylation as a mechanism involved in plant protection to
52 environmental stresses. In addition, the designed strategy allows its implementation in
53 important crop plants regardless of its genetic complexity, and other non-plant organisms.

54

55

2

INTRODUCTION

In response to external and internal cues, plants develop finely tuned growth programs adapted to environmental conditions and developmental stage (Naseem et al., 2015). Protein post-translational regulation by SUMO conjugation has emerged as a major molecular mechanism regulating plant growth and stress responses. As ubiquitin, SUMO is attached to protein targets through sequential reactions catalyzed by the E1, E2 and E3 enzymes (Gareau and Lima, 2010). SUMO proteases are responsible for SUMO maturation and deconjugation (Gareau and Lima, 2010).

SUMO activation is a two-step ATP-dependent reaction catalyzed by the heterodimeric E1-activating enzyme, SAE2/SAE1, which is the first control point to enter the conjugation cascade (Supplemental Figure 1)(Castaño-Miquel et al., 2011; Walden et al., 2003). SAE2 is structured in four functional domains: adenylation, catalytic cysteine (SAE2^{Cys}), ubiquitin-fold (domain structurally resembling ubiquitin, SAE2^{UFD}) and C-terminal (SAE2^{Ct}) domains (Lois and Lima, 2005). The E1 activating enzyme small subunit, SAE1, contributes the essential Arg21 to the adenylation domain (Lee and Schindelin, 2008). The adenylation domain is responsible for SUMO recognition and SUMO C-terminus adenylation. After adenylation, the SUMO C-terminal adenylate establishes a thioester bond with the E1 catalytic cysteine. Following thioester bond formation, SUMO can be transferred to the E2-conjugating enzyme in a reaction that involves E2 recruitment through the two interacting surfaces (Lois and Lima, 2005; Reiter et al., 2015; Wang et al., 2007; Wang et al., 2010) (Figure 1A). On one hand, the SAE2^{UFD} domain establishes contacts with residues located at the α1-helix and the β1β2-loop of the E2 conjugating enzyme (Reiter et al., 2015; Wang et al., 2009; Wang et al., 2010). On the other, the SAE2^{Cys} domain interacts with residues located at the E2 α4 N-terminus (Wang et al., 2007). Although both interactions surfaces involved SAE2 residues present in loops, SAE2^{UFD}-E2 interactions display higher affinity (K_d = 1.2 μM)(Reiter et al., 2013) than SAE2^{Cys}-E2 interactions (K_d = 80 μM)(Wang et al., 2007), supporting a major role of the SAE2^{UFD} domain in E2 recruitment. Even though the SAE2^{UFD} domain is essential in yeast (Lois and Lima, 2005), it remains unclear whether SAE2^{UFD} is sufficient for efficient E2 recruitment *in vivo*.

In plants, SUMOylation has been shown to modulate plant hormone signaling (Conti et al., 2014; Lois et al., 2003; Miura et al., 2009), root stem cell maintenance (Xu et al., 2013), and responses to abiotic and biotic stress (Lois, 2010). Many of the plant biological processes regulated by SUMOylation have been uncovered by the analysis of proteases and SUMO E3 ligase mutant plants, which display pleiotropic growth defects and reduced viability (Huang et

92 al., 2009; Ishida et al., 2009; Miura et al., 2005; Murtas et al., 2003). Nonetheless, some of
93 these mutations have also been proposed to confer adaptive responses to some stresses,
94 such as salt, drought, resistance to plant viruses and salicylic acid-mediated plant immunity
95 (Lee et al., 2007; Miura et al., 2013; Miura et al., 2011; Saleh et al., 2015; Yoo et al., 2006).
96

97 Despite the important agronomic traits regulated by SUMO, most of research studies on
98 SUMOylation have been mainly limited to model plants, such as *Arabidopsis* and rice (Wang
99 et al., 2011), due to the lack of molecular tools specific to other economically relevant plants.
100 On the other hand, plants harboring mutations in main components of the SUMOylation
101 machinery, such as *Arabidopsis siz1 (Miura et al., 2010), mms21 (Huang et al., 2009; Ishida
102 et al., 2009) or esd4 (Murtas et al., 2003)*, display severe growth defects that are dependent
103 on SA accumulation (Miura et al., 2010; Villajuana-Bonequi et al., 2014). For overcoming
104 these technical constraints, developing tools alternative to null mutants are of great interest.
105

106 Considering the relevance of SUMO as a major post-translational modification, it is expected
107 that novel biological functions regulated by SUMO remain to be uncovered. Necrotrophic
108 pathogens, such as *Botrytis cinerea* and *Plectosphaerella cucumerina*, promote host cell
109 death to acquire nutrients for proliferation on dead and decaying tissues. Defense responses
110 regulated by SA-dependent pathway and associated to programmed cell death are effective
111 against biotrophic pathogens, however, they benefit necrotrophic pathogens. Control of
112 necrotroph infections is achieved by a different set of defense responses activated by
113 jasmonic acid and ethylene signaling (Glazebrook, 2005). Despite recent progress,
114 knowledge of how plants perceive and respond to necrotrophy is behind our understanding
115 of plant responses to biotrophy (Mengiste, 2012).
116

117 Here, we have developed an innovative strategy for inhibiting SUMO conjugation *in vivo* as
118 an alternative to knock-out mutants, which are lethal, in case of E1-activating and E2-
119 conjugating enzymes, or display strong pleiotropic phenotypes, in case of E3 ligases. We
120 have shown that SAE2^{UFDCt} functions as a SUMO conjugation inhibitor both *in vitro* and *in
121 vivo* in a dose-dependent manner, through a mechanism based on its ability to establish non-
122 covalent interactions with the SUMO E2-conjugating enzyme. Our results showed that the
123 SAE2^{UFDCt} domain is sufficient for E2 recruitment *in vivo*, providing a novel molecular target
124 for developing small molecule SUMO conjugation inhibitors. SAE2^{UFDCt} expression is robust
125 and stable through plant generations and it has allowed uncovering a novel post-
126 transcriptional regulation of *in vivo* SUMO E2-conjugating enzyme levels. In addition, the
127 study of these plants has facilitated the identification of a novel role of SUMO in defense
128 responses against necrotrophic fungal pathogens. The use of SAE2^{UFDCt} expressing lines

129 have provided an advantage over the use of *siz1* E3 ligase knock-out mutants by allowing
130 the analysis of plant susceptibility to fungal pathogens under different degrees of
131 SUMOylation inhibition. Our results indicate that SUMOylation is required for resistance to
132 necrotrophic fungal attacks. During infection, free- and conjugated-SUMO, the E1-activating
133 enzyme large subunit SAE2, and the E2-conjugating enzyme SCE1 diminished. In summary,
134 we provide a novel strategy for SUMOylation inhibition that is easy to implement in any
135 transformable plant regardless of its genetic complexity, and we have validated it by
136 uncovering a novel regulatory role of SUMO in defense responses to necrotrophic fungi. Our
137 findings suggest that depleting host SUMO conjugation machinery could constitute a novel
138 mechanism for fungal pathogenicity.
139

140 **RESULTS**

141 **SAE2^{UFDCt} is essential for Arabidopsis SUMO E1 activity and, as independent domain,**

142 **inhibits SUMO conjugation.**

143 In order to develop an innovative strategy for inhibiting SUMOylation that could be easily

144 implemented in any transformable organism of interest, plant or animal, we have exploited

145 the disruption of SUMO E1-activating and E2-conjugating enzyme interactions (Figure 1A).

146 Previous studies identified two independent regions in the SUMO E1 large subunit SAE2

147 involved in E2 interactions located at the SAE2 Cys and UFD domains, respectively. We

148 performed comparative analyses of SAE2 protein orthologs from human, yeast and

149 Arabidopsis, and found that SAE2 regions involved in E2 interactions exhibited a

150 conservation degree from 2-fold to 6-fold lower than the conservation displayed by the SAE2

151 domains in which they are contained, the full UFD or full Cys domains, respectively

152 (Supplemental Figure. 2). This localized divergence suggests that these regions, which we

153 have named LHEB1 and 2 (Low Homology region involved in E2 Binding 1 and 2), have

154 optimized cognate interactions across evolution. From the E2 side, the region involved in

155 SAE2 binding is better conserved across species and it also participates in SUMO non-

156 covalent interactions (Wang et al., 2010), which are necessary for polySUMO chain

157 formation (Capili and Lima, 2007; Castaño-Miquel et al., 2011; Knipscheer et al., 2007). In

158 order to avoid interfering with protein-protein interactions other than E1-E2 interactions, we

159 designed a strategy based on SAE2^{UFDCt} domain engineering. The SAE2^{UFDCt} domain

160 includes residues from Ser436 to Glu625. In SUMO conjugation assays *in vitro*, the

161 *Arabidopsis* SAE2^{UFDCt} domain is essential for SUMO conjugation and, when included as an

162 independent domain in the assays, the SAE2^{UFDCt} domain displayed the capacity to inhibit

163 SUMO conjugation in a dose-dependent manner (Figure 1C and D). The SAE2^{UFDCt} domain

164 was also competent to inhibit SUMOylation of SCE1, which further supports the role of the

165 SAE2^{UFDCt} domain in the direct disruption of E1-E2 interactions (Supplemental Figure 4).

166

167 **The SAE2^{UFDCt} LHEB2 region has a major role in SAE2^{UFDCt}–SCE1 non-covalent**

168 **interactions.**

169 Previous structural studies suggested that yeast LHEB2 establishes hydrophobic and ionic

170 interactions with Ubc9 (yeast SUMO E2 enzyme), which involve a Leu and two Asp residues,

171 respectively (Wang et al., 2010). Due to the low homology between *Arabidopsis* and yeast

172 LHEB2 regions (6% of sequence identity), it was not possible to unequivocally identify the

173 corresponding functional residues in *Arabidopsis* SAE2. Instead, we performed comparative

174 analyses of LHEB2 domain conservation among plant SAE2 orthologs and their

175 corresponding UFD domain assigned according to sequence homology. The identified

176 SAE2^{UFD} sequences were re-aligned and the resulting alignment was used to perform

6

177   phylogenetic analyses of the UFD domain (Supplemental Figure 3A) or the LHEB2 domain

178   (Figure 2A) sequences. The resulting parsimony phylogenetic trees showed that the

179   evolutionary relationships among the SAE2^{UFD} domain sequences were consistent with

180   taxonomic lineages. On the contrary, when evolutionary relationship between LHEB2

181   sequences was analyzed, the resulting clades were not consistent with taxonomic lineages

182   (Supplemental Figure 3B, C), supporting the hypothesis that the LHEB2 domain has

183   undergone higher diversification than the overall SAE2 sequence. The LHEB2 consensus

184   sequence was determined for angiosperms, lower plants and algae (Figure 2B), and their

185   comparative analysis showed that the LHEB2 domain displayed differences in sequence

186   length and composition among these evolutionary groups.

187

188   From the angiosperm LHEB2 consensus sequence, we selected hydrophobic and acidic

189   amino acid residues that could potentially be involved in E2 binding according to previous

190   reports in yeast (Wang et al., 2010) (Figure 2B and Supplemental Figure 2). To analyze the

191   role of the selected residues in E2 binding, we introduced four single mutations into

192   SAE2^{UFDCt}, L476A, L477A, D485A and D486A, and tested their effect in SAE2^{UFDCt}-E2

193   interactions in pull down assays *in vitro*. All SAE2^{UFDCt} mutant forms were impaired in E2

194   binding, although this defect was more prominent in L476A and D485A mutant forms (Figure

195   2C and D). These results were consistent with a major role of polar and hydrophobic

196   interactions in E2 binding. Also, these results showed that amino acid residues comprised in

197   SAE2^{UFDCt} LHEB2 are crucial for establishing SUMO E1-E2 interactions.

198

199   **Constitutive SAE2^{UFDCt} domain expression confers attenuated developmental defects**

200   **displayed by SUMOylation impaired plants.**

201   In order to test the capacity of the SAE2^{UFDCt} domain to inhibit SUMO conjugation *in vivo*, we

202   generated plants expressing *Arabidopsis* SAE2^{UFDCt} domain under the control of the CaMV

203   35S promoter. Among the obtained transgenic plants, three independent lines expressing

204   from lower to higher levels of SAE2^{UFDCt}, #28, #1 and #44, were selected for further

205   characterization (Figure 3A top). In these plants, accumulation of SUMO conjugates was

206   diminished in direct relationship to SAE2^{UFDCt} expression levels (Figure 3B, Supplemental

207   Figure 5). As controls, we included Col0 and *siz1-3* mutant plants, which displayed the

208   highest and the lowest SUMO conjugate accumulation levels among the analyzed lines,

209   respectively. Remarkably, SCE1 levels were significantly increased in these plants (Figure

210   3A bottom), and this increment was proportional to SAE2^{UFDCt} expression levels. In contrast,

211   SAE2 endogenous levels were not altered. The analysis of mRNA SCE1 levels revealed no

212   significant differences between SUMOylation impaired plants and control Col0 plants

213 (Supplemental Figure 7), suggesting that regulation of endogenous SCE1 protein levels
214 would involve a novel post-transcriptional mechanism.

215

216 The phenotypic analysis showed that SAE2^{UFDCt} expressing plants displayed developmental
217 alterations present in SUMOylation deficient plants, such as reduced plant size (Figure. 3C
218 and D), early flowering (Figure. 3E) and reduced seed yield (Figure. 3F)(Lois, 2010). The
219 extent of these alterations was consistent with a gradual SUMO conjugation inhibition
220 between the different transgenic lines and it was maintained through generations. In addition,
221 SAE2^{UFDCt} expression impaired desiccation-induced SUMO conjugate accumulation and
222 conferred plant susceptibility to drought (Supplemental Figure 6), both responses
223 characteristic of the SUMO E3 ligase mutant *siz1-3* (Catala et al., 2007).

224

225 At molecular level, we characterized the capacity of SAE2^{UFDCt} to interact with SCE1 as a
226 mechanism of SUMO conjugation inhibition. In transient expression experiments in onion
227 cells, SCE1 localized to the nucleus and the cytosol, while the SAE2^{UFDCt} domain localized
228 exclusively to the nucleus, which is consistent with the presence of a nuclear localization
229 signal in the SAE2 C-terminal tail (Castaño-Miquel et al., 2013). When SAE2^{UFDCt} and SCE1
230 were co-expressed, SCE1 localized exclusively to the nucleus, suggesting that the SCE1
231 cytosolic fraction was recruited to the nucleus by SAE2^{UFDCt} (Figure 4A). To further test the
232 SAE2^{UFDCt}-E2 interactions *in vivo*, we performed immunoprecipitation assays in protein
233 extracts from line #44 of SAE2^{UFDCt} expressing plants. The SUMO-E2 conjugating enzyme
234 SCE1 was specifically co-immunoprecipitated when anti-SAE2 antibodies were used, but not
235 in presence of pre-immunization antibodies, further supporting that the SAE2^{UFDCt} domain is
236 competent for E2 recruitment *in vivo* (Figure 4B).

237

238 ***Plants with impaired SUMOylation exhibit enhanced susceptibility to fungal pathogen***
239 ***infection.***
240 In order to further validate the developed strategy for inhibiting SUMO conjugation *in vivo*, we
241 investigated a novel role of protein SUMOylation in plant defense against fungal pathogens.
242 For this purpose, several Arabidopsis genotypes with altered SUMOylation activity were
243 challenged with two different necrotrophic pathogens, namely *Botrytis. cinerea* and
244 *Plectosphaerella cucumerina*. The selected plants accounted for increased SUMOylation,
245 SUMO1-ox plants (Lois et al., 2003), and diminished SUMOylation, including SUMOylation
246 deficient SAE2^{UFDCt} expressing plants lines #28, #1 and #44, and *siz1-3* mutant plants. The
247 progress of diseases was macroscopically examined and compared to wild-type plants.
248 Disease lesions caused by *B. cinerea* were first visible as discrete necrotic spots at 2 dpi in
249 those lines impaired in SUMOylation, whereas, in the wild-type and *SUM1*-ox leaves,

8

necrosis appeared later, at 3 dpi (Figure 5A). These lesions expanded and caused maceration on the inoculated leaves in the next few days, developing more quickly on the *siz1-3* and the *SAE2^{UFDCt}* expressing lines (Figure 5A). At 15 dpi, most of inoculated *siz1-3* mutant and transgenic plants from lines #1 and #44 were dead, whereas most of the wild-type, *SUM1*-ox and line #28 plants remained alive and survived to the disease under these experimental conditions (Figure 5B). These results suggest that protein SUMOylation is required for resistance to *B. cinerea* fungal infection. Similarly, the plants impaired in SUMOylation showed enhanced susceptibility to the fungal pathogen *P. cucumerina,* as they displayed necrosis on the majority of leaves at 7 dpi (Figure 5C) that expanded through the petioles and reached the vascular system causing around a 50% decay of plants at 10 dpi (Figure 5D). This phenotype differed to the moderate susceptibility shown by the wild-type and *SUM1*-ox plants, in which necrotic spots in most of the leaves were observed, but complete necrosis only developed in basal leaves, and most of the inoculated plants survived (Figure. 5C, D). In these experiments, the *agb1-1* mutant (Llorente et al., 2005), which displays an enhanced susceptibility to *P. cucumerina*, was used as positive control of fungal infection. These macroscopic disease symptoms were associated to a higher fungal growth on *siz1-3* or *SAE2^{UFDCt}* leaves, as revealed by trypan-blue staining of fungal hyphae (Figure 5E). The SUMOylation deficient leaves and the *agb1-1* mutant supported an increased fungal growth, consistent with the displayed plant susceptibility. The *SUM1*-ox and wild-type plants with high and basal SUMOylation profiles, respectively, showed moderate susceptibility, whereas the *SAE2^{UFDCt}* lines and *siz1-3* mutant plants with reduced SUMOylation conjugates showed high susceptibility to *P. cucumerina* (Figure. 5F).

In order to better understand the requirement of SUMOylation for necrotrophic pathogen resistance, we analyzed the molecular dynamics of SUMO, free and conjugated, and two members of the SUMOylation machinery, the SUMO-activating enzyme large subunit SAE2 and the SUMO-conjugating enzyme SCE1, during *P. cucumerina* infection of wild type Col0 plants. At 3 hpi, a transient and significant increment in SUMO conjugates was observed. Then, a gradually reduction of SUMO conjugates was observed, reaching a 50% reduction at 48 hpi, which did not correlate with an accumulation of free SUMO. On the contrary, free SUMO levels were also reduced during infection (Figure 6A, C), indicating that the reduction of SUMO conjugates is not consequence of active deconjugation. Similarly, SAE2 and SCE1 protein levels diminished during infection, although with slightly different dynamics. SCE1 levels were gradually reduced, whereas SAE2 levels were maintained up to 24 hpi and then reduced at 48 hpi (Figure 6A, D, E). After 7-dpi, dead plants were clearly observed (Supplemental Figure. S8). The analysis of mRNA SUMO1, SAE2 and SCE1 levels did not reveal fluctuations that would account for the reduction in protein levels (Figure.6B). These

9

287   results suggest that reduction of SUMO, SAE2 and SCE1 protein levels in response to

288   necrotrophic fungal infection is post-transcriptionally controlled.

289

290 **DISCUSSION**

291 Taking advantage of the highly specific protein-protein interactions among cognate enzymes

292 that mediate SUMO conjugation to substrates, we have developed a novel strategy for

293 achieving inhibition of SUMO conjugation *in vivo* based on disruption of SUMO E1-E2

294 interactions. We have validated this strategy for uncovering a novel role of SUMO

295 conjugation in defense responses to necrotrophic fungal pathogens.

296

297 *Structure-based SUMO conjugation inhibition*

298 Since SUMOylation is an essential process, the use of knock-out mutants affecting the first

299 steps in the SUMO conjugation pathway, such as the E1-activating or the E2-conjugating

300 enzymes, is compromised. As a result, the use of knock-out mutants has been limited to the

301 study of specific E3- ligases-depending functions, such as SIZ1 or MMS21, which are the

302 only SUMO E3-ligases described in *Arabidopsis*. Null *siz1* and *mms21* mutant plants display

303 dramatic pleiotropic growth defects (Ishida et al., 2009; Miura et al., 2010), which could raise

304 concerns about the direct role of SUMO in the reported biological functions. In addition, the

305 dependency of the *siz1* phenotype on growth conditions have generated contradictory

306 observations regarding its role in drought responses (Catala et al., 2007; Miura et al., 2013),

307 accentuating the need for alternative genetic tools. The strategy that we have developed

308 renders plants without compromised viability and facilitates the study of physiological

309 processes over a range of SUMOylation inhibition, establishing dose-dependent responses.

310 Both aspects constitute an advantage over the use of null E3 ligases mutants.

311

312 Previous attempts aimed to inhibit *in vivo* SUMOylation by expressing a SUMO E2-inactive

313 mutant, but resulted in transgene silencing after few generations (Lois et al., 2003; Tomanov

314 et al., 2013). In contrast, the expression of the SAE2^{UFDCt} domain is maintained through

315 generations. In addition, inhibition of protein functions has some advantages over applying

316 RNA interference approaches such as, avoiding off-target effects (Jackson and Linsley,

317 2010) and, it is easier to implement in species with high genome complexity, as some crops,

318 than approaches involving multiple knock-out or knock-down mutant generation. Considering

319 the mentioned aspects, SAE2^{UFDCt} expression is a reliable and novel approach to inhibit

320 SUMO conjugation *in vivo* that could contribute to accelerate our knowledge of how SUMO

321 regulates traits affecting productivity of important crops.

322

323 *New mechanistic insights into in vivo SUMO conjugation*

324 To our knowledge, this is the first report describing that the disruption of SUMO E1 –E2

325 interactions is a valid strategy for inhibiting SUMO conjugation *in vivo* and supports a major

326 role for the SAE2^{UFDCt} domain in E2-recruitment *in vivo*. Disruption of protein-protein

327 interactions potentially offers advantages over single enzyme inhibition related to increased
328 affinity and specificity (Zinzalla, 2013). Accordingly, the low conservation displayed by the
329 LHEB2 sequences suggests that these regions have evolved to optimize E1-E2 cognate
330 interactions. Supporting this hypothesis, previous studies performed by us and others
331 showed that the *in vitro* efficiency of the human SUMO conjugation system was dramatically
332 reduced when the human E2-conjugating enzyme was replaced by the *Arabidopsis (Lois et*
333 *al., 2003)* or the *Plasmodium falciparum (Reiter et al., 2013)* SUMO E2 orthologs. Also, as
334 result of this divergence, identifying the specific amino acids displaying a major contribution
335 to these interactions is not possible by sequence homology between evolutionary distant
336 organisms, such as yeast and plants. By using mutagenesis analysis, we have identified
337 residues necessary for SAE2^{UFD}-E2 interactions that are present with a high frequency in the
338 angiosperm SAE2 sequences analyzed, but not in lower plants, consistently with the
339 proposed higher divergence rate of this region.

340

341 In addition, we have uncovered a novel post-transcriptional regulation of SUMO E2 levels,
342 which accumulate in a direct relation to the SAE2^{UFDCt} expression levels. Previous studies
343 reported an accumulation of the E2 in *siz1* mutant plants and suggested the existence of a
344 compensatory mechanism that was not analyzed (Saracco et al., 2007). We have observed
345 similar E2 accumulation in *siz1* mutant plants, but this accumulation was much higher in
346 SAE2^{UFDCt}-expressing plants, even though they displayed less dramatic defects in SUMO
347 conjugate accumulation than *siz1* mutant plants. This is particularly evident in the case of the
348 transgenic line expressing the lowest SAE2^{UFDCt} levels, line #28, which had a minor effect on
349 SUMO conjugate accumulation and, consequently, plants did not display obvious
350 developmental defects under standard growth conditions. These results provide evidences
351 for the existence of an unknown *in vivo* SUMOylation regulation mechanism based on
352 controlling E2 levels. We speculate that the SCE1-SAE2^{UFDCt} complex could mediate SCE1
353 stabilization. *In planta*, such mechanism could facilitate the coordination between E1 and E2-
354 levels in order to modulate SUMO conjugation rate.

355

356 *SUMOylation is required for resistance to plant necrotrophic fungal pathogens.*
357 In the last years, post-translational modification mechanisms have emerged as key players in
358 the plant defense responses to pathogens. The role of phosphorylation, ubiquitination,
359 sumoylation, nitrosylation and glycosylation has been described in plant immunity (Lee et al.,
360 2007; Stulemeijer and Joosten, 2008). Since previous studies did not identify alterations in
361 *siz1* mutant plants susceptibility to necrotrophic pathogens, we evaluated a potential role of
362 SUMO in this process that could potentially be SIZ1-independent. We found that transgenic
363 plants expressing the SAE2^{UFDCt} domain displayed increased sensitivity to the tested fungi.

364 Surprisingly, when we included *siz1* mutant plants in the assays, we observed that they also
365 displayed sensitivity to necrotrophic fungal pathogens. Response variability of *siz1* mutant
366 plants upon stress was previously observed in drought tolerance studies (Catala et al., 2007;
367 Miura et al., 2013), stressing the need for alternative and more reliable approaches to study
368 the role of SUMOylation in plants, as the strategy described here. In fact, SAE2[UFDCt]
369 expressing plants also displayed increased drought sensitivity, supporting Catala and co-
370 workers findings.

371

372 Defense responses regulated by SA-dependent pathway and associated to programmed cell
373 death, which are effective against biotrophic pathogens, benefit necrotrophic pathogens. The
374 null *siz1* mutant plants are characterized by high contents of SA, which results in higher
375 expression of PR genes inducing a constitutive systemic-acquired resistance (SAR) leading
376 to an increased resistance to the bacterial pathogen *Pseudomonas syrinage pv.tomato (Pst)*
377 *(Lee et al., 2007; van den Burg et al., 2010).* Therefore, the *siz1* susceptibility to necrotrophic
378 pathogens that we observed is consistent with SA accumulation in these plants.

379

380 To further understand the role of SUMOylation in pathogen defense, we determined protein
381 dynamics of SUMO conjugation machinery members, SUMO E1-activating enzyme large
382 subunit, E2-conjugating enzyme and free- and conjugated- SUMO, during the first 48h post-
383 infection, when physical damage was not observed. Although the different components follow
384 distinct dynamics, at 48hpi, a general depletion of the SUMOylation system was observed,
385 which did not correlate with significant alterations in mRNA levels, suggesting the existence
386 of a post-transcriptional regulation. Since SUMOylation inhibition results in cell death (Miura
387 et al., 2010), it is plausible that necrotroph fungi could induce SUMOylation machinery
388 depletion as a mechanism of pathogenicity. Supporting this hypothesis, it is well described
389 the role of some bacterial pathogen effectors targeting the host SUMOylation machinery. As
390 such, the *Xanthomonas campestris* effectors XopD and AvrXv4 act as SUMO proteases
391 (Chosed et al., 2007) resulting in the disruption of SUMO homeostasis in the cell (Hotson
392 and Mudgett, 2004; Roden et al., 2004), which favors infection progression. In viral
393 infections, the essential proteins for viral replication AL1 and REP interact with SUMO E2-
394 conjugation enzyme, altering the cell SUMO conjugation capacity (Castillo et al., 2004;
395 Sanchez-Duran et al., 2011). This manipulation of SUMOylation machinery by pathogens is a
396 strategy also present in animal viruses and bacteria (Beyer et al., 2015; Boggio et al., 2007;
397 Ribet et al., 2010). The existence of similar strategies used by fungi during host infections
398 remains to be elucidated.

399

400 Overall, we have validated the disruption of SUMO E1 and E2 interactions as a reliable
401 strategy for inhibiting SUMO conjugation *in vivo,* that could be applied to accelerate the
402 understanding of SUMOylation in organisms for which genetic tools are not available, such
403 as economically relevant crops. Also, this validation constitutes a starting point to develop
404 novel agrochemicals for selective modulation of plant stress responses such as plant
405 immunity. Finally, we have shown the advantage of this strategy over the use of null mutants,
406 which sometimes deliver contradictory results, by identifying a novel role of SUMO in
407 defense responses against necrotrophic fungal pathogens. Additional studies will be
408 necessary to elucidate the molecular mechanisms involved in SUMO conjugation machinery
409 depletion during fungal infection.

410

14

411 **MATERIAL AND METHODS**

412 *Plant Material and Growth Conditions.* For *in vitro* cultures, seeds were stratified for 3 days,

413 plated on Murashige and Skoog salts (Duchefa), pH 5.7, supplemented with 0.8% BactoAgar

414 (Difco), and transferred to a tissue culture room in a LD photoperiod (16 h light/8 h dark) at

415 22 ℃. For soil cultures, plants were grown in growth chambers in a LD photoperiod at 22ºC.

416 For immunoprecipitation assays, seedlings of SAE2^{UFDCt} expressing line #44 were

417 germinated and grown in Gamborg liquid medium for 11 days in constant agitation (120 rpm)

418 in a LD photoperiod (16h light/8h dark) culture room. Plants were immediately frozen with N$_2$

419 and stored at -80℃.

420

421 *In Vitro SUMO conjugation.* A detailed protocol for reconstituting an in vitro SUMO

422 conjugation assay

423 covering all steps from protein preparation to assay development and kinetics quantification

424 is described in (Castaño-Miquel and Lois, 2016). Briefly, in conjugation assays, we used the

425 C-terminal tail of the Arabidopsis Catalase 3 (419-472) fused to GST, GST:AtCAT3Ct as a

426 substrate. Reactions were carried out at 37ºC in 25 μL reaction mixtures containing 1 mM

427 ATP, 50 mM NaCl, 20 mM Hepes, pH 7.5, 0.1% Tween 20, 5 mM MgCl$_2$, 0.1 mM DTT, 2 μM

428 SUMO, 0.5 μM AtSAE2/AtSAE1a, 0.5 μM AtSCE1 and 5 μM GST-AtCAT3Ct. After the

429 specified incubation time, reactions were stopped by the addition of protein-loading buffer,

430 incubated at 70 ºC for 10 min, and 10 μL aliquots were resolved by SDS-PAGE. Reaction

431 products were detected by immunoblot analysis with anti-GST polyclonal antibodies (SIGMA,

432 G7781). Luminescence signal generated by ECL Prime assay (GE Healthcare) was captured

433 with a CCD camera (LAS4000, Fujifilm) and quantified with Multigauge software (Fujifilm). In

434 order to remove variability resulting from antibodies incubations and time exposure

435 differences, each data point was normalized to the average of all data points obtained from

436 each analyzed membrane. The normalized values were used to calculate the corresponding

437 slopes (relative luminescence signal versus time). The average slope from at least three

438 independent experiments is shown.

439

440 *In vitro pull-down assay.* 100 μM His:AtSAE2^{UFDCt} or its mutant variants L476A, L477A,

441 D485A and D486A, and 25 μM of AtSCE1 were incubated in 40 μL of binding buffer (50 mM

442 Tris pH 8.0, 150 mM NaCl and 20 mM imidazol) for 1 hour at 4ºC. Next, 10 μL of Ni^{2+}-IMAC-

443 sepharose resin were added to the binding mixture and incubated for 30 minutes at 4ºC. The

444 binding mixture was transferred to micro bio-spin chromatography columns (BIO-RAD, 732-

445 6203) and the resin was washed three times with 20 μL of binding buffer and a final wash of

446 40 μL of binding buffer. The proteins bound to the resin were eluted with 20 μL of binding

15

447 buffer containing 300 mM imidazol. 0.5 μL of the input and 1 μL of the eluate fractions,
448 respectively, were separated by SDS-PAGE and subjected to immunoblot analysis with anti-
449 SCE1 antibodies.

450

451 *Transient Expression of Fluorescent Protein Fusions in Onion Cells.* SAE2^{UFDCt} and SCE1
452 were fused in frame to the 3' end of the coding sequences of yellow fluorescent protein
453 (YFP) or cyan fluorescent protein (CFP), respectively, downstream of the 35S constitutive
454 promoter. Onion epidermal cells were bombarded with 5 μg of each DNA construct using a
455 helium biolistic gun (BIO-RAD). Treated epidermal cells were kept in the dark at room
456 temperature for 16 h before analysis by confocal microscopy (Confocal Olympus FV 1000).
457 YFP was excited with a 515-nm argon laser and images collected with a 550- to 630-nm
458 range. CFP was excited with a 405-nm argon laser and images collected in the 460- to 500-
459 nm range. Imaging of YFP and CFP imaging and transmissible light images collection were
460 performed sequentially. Samples were scanned with the Z-stack mode and image stacks
461 projection was calculated with ImageJ software (Rasband, 1997-2009).

462

463 *Protein extraction and immunoblot.* Anti-SUMO1/2, anti-SAE2 and anti-SCE1 polyclonal
464 antisera were generated previously(Castaño-Miquel et al., 2011). Plant tissue was ground in
465 liquid nitrogen and proteins extracted with 50 mM Tris-HCl pH 8, 150 mM NaCl, 0.2% Triton
466 X-100, 1 mM PMSF, 1 μg/mL pepstatin, 1 μg/mL leupeptin, 2 mM *N*-ethylmaleimide, 10 mM
467 iodoacetamide; 5 mM EDTA. 18μg of total protein were resolved under reducing conditions
468 by using SDS polyacrylamide gels and NuPage Novex 4-12% Bis/Tris Gels (Invitrogen).
469 Proteins were transferred onto polyvinylidene difluoride (PVDF) membranes (Millipore),
470 incubated overnight with primary antibody, followed by secondary antibody incubation,
471 peroxidase-conjugated anti-rabbit (GE Healthcare), for 1h at room temperature in TBST (20
472 mM Tris-HCl at pH 7.6; 20 mM NaCl, 0.1% (v/v) Tween20) supplemented with 3% non-fat
473 dry milk. Peroxidase activity was developed in ECL Plus reagent (GE Healthcare) and
474 chemiluminescence signal captured with LAS-4000 imaging system (Fujifilm). For SUMO
475 conjugate quantifications, using Multigauge v.3 (Fujifilm), the region of interest (ROI) was
476 defined by a rectangle enclosing all detected bands above free SUMO in each lane. The
477 same ROI size was used for quantifying SUMO conjugates from each sample lane and the
478 membrane background. Average values were calculated as described in (Castaño-Miquel
479 and Lois, 2016).

480

481 *Phylogenetic analyses.* We searched Phytozome v.11 for Arabidopsis SAE2 homologs and
482 retrieved one hundred sequences. Before performing comprehensive homology analysis,
483 incomplete sequences were removed. When different versions of the same gene were

16

found, we retained the version containing all the canonical SAE2 functional regions for the comparative analysis. The remaining sixty SAE2 homolog proteins from fifty-four plant species were aligned using the OMEGA clustal software (http://www.ebi.ac.uk/Tools/msa/clustalo/) and the human SAE2 as outlier. Phylogenetic analysis was performed using Seaview software. Consensus sequences were calculated using WebLogo software (http://weblogo.berkeley.edu/)(Crooks et al., 2004). Multiple sequence alignments were edited, analyzed and shaded using GeneDoc(Nicholas and Nicholas, 1997).

Immunoprecipitation assays. 1 g of 11-day old Arabidopsis seedlings were ground and homogenized in 2 ml of immunoprecipitation (IP) buffer (50 mM Tris-HCl pH 7.5, 100 mM NaCl, 0.2% Triton X-100, 1 mM DTT, 1 µg/mL pepstatin, 1 µg/mL leupeptin, 2 mM *N*-ethylmaleimide, 10 mM iodoacetamide and 5 mM EDTA), incubated for 30 min rotating at 4℃ and centrifuged at 14.000 x g for 20 minutes at 4℃. Supernants were recovered and concentrated with centrifugal filters (Amicon Ultra-15 10kDa), and subsequently quantified using the Bradford assay (Bio-Rad Protein Assay). 12 mg of total protein were incubated for 3h at 4℃ on a rotator in the presence of 30 µL of SAE2 polyclonal antiserum, or 90 µL of the corresponding pre-immunization serum, and 50 µL of Protein A Magnetic Beads (Surebeads, Bio-Rad). After three washes with IP buffer, immunoprecipitated proteins were eluted by boiling at 100ºC in Laemmli buffer and analyzed by immunoblotting using anti-SAE2 and anti-SCE1 antibodies. As control, 5 µg of input fractions were also analyzed.

RNA Extraction and Quantitative Real-Time RT-PCR. Total RNA from plant tissues was extracted using the Maxwell 16 LEV simplyRNA Tissue Kit (Promega, Wisconsin, USA) according to the manufacturer's instructions. The Superscript VILO kit (Invitrogen, Massachusetts, USA) was used to generate cDNA according to the manufacturer's instructions, using 1.4 µg of total RNA. The relative mRNA abundance was evaluated via quantitative reverse transcription PCR (RT-qPCR) in a total reaction volume of 20 µl using LightCycler 480 SYBR Green I Master (Roche, Basel, Switzerland) on a LightCycler 480 Real-Time PCR System (Roche, Basel, Switzerland) with 0.3 µM of each specific sense and anti-sense primers. Two or three independent biological replicates of each sample, as stated in the text, and three technical replicates of each biological replicate were performed and the mean values were considered for further calculations. The relative transcript level was determined for each sample and normalized using *UBC21* or *PR65* as stated. Primer sequences used in the qPCR experiments are described in Supplemental Table II.

Infection assays. The *Botrytis cinerea* and *Plectosphaerella cucumerina* fungal strains, as well as the Arabidopsis mutant *agb1-1* showing high susceptibility to *P. cucumerina* infection[1], were provided by Dr. A. Molina (CBGP, Spain). Plants were grown in a phytochamber on a sterilized mixture of soil and vermiculite (3:1) during 4 weeks under a 12 h light/12 h dark photoperiod at 22°C prior inoculation. Inoculated plants were kept under high humidity in covered trays. *B. cinerea* inoculations were performed by placing spore suspension drops (10^6 spores/ml) on Arabidopsis leaves (4 leaves per plant). *P. cucumerina* inoculations were performed spraying plants with spore suspensions (10^5 spores/ml). At least 8 plants per genotype were inoculated in a minimum of 2 or 3 independent assays. Disease progression was followed by visual inspection. Fungal growth was visualized by trypan blue staining of leaves at 2 and 3 dpi as reported[2], and bright field images were obtained on a Zeiss Axiophot microscope.

Accession numbers. Assigned accession numbers for the genes used in this work are as follows: At5g55160 (SUMO2), At2g21470 (SAE2), At4g24940 (SAE1a), At3g57870 (SCE1), PR65 (At1g13320).

Author Contribution

LCM, AM, IT, AP, BT, JS, ALS, NR, GLV, SM, MC and LML performed experiments. LCM, AM, IT, AP, ALS, SM, MC and LML designed experiments. MC supervised experiments involving fungal infections. LML supervised and led this project. MC and LML wrote the manuscript. LCM, AM, IT, AP, ALS, SM, MC and LML discussed and checked the manuscript. All authors contributed to the analysis of the data and approved the manuscript.

Acknowledgments

Conflict of Interest

The authors declare that they have no conflict of interest

557 **REFERENCES**

558 Beyer, A.R., Truchan, H.K., May, L.J., Walker, N.J., Borjesson, D.L., and Carlyon, J.A.
559   (2015). The Anaplasma phagocytophilum effector AmpA hijacks host cell
560   SUMOylation. Cell Microbiol 17:504-519.

561 Boggio, R., Passafaro, A., and Chiocca, S. (2007). Targeting SUMO E1 to ubiquitin ligases: a
562   viral strategy to counteract sumoylation. J Biol Chem 282:15376-15382.

563 Capili, A.D., and Lima, C.D. (2007). Structure and analysis of a complex between SUMO and
564   Ubc9 illustrates features of a conserved E2-Ubl interaction. J. Mol. Biol. 369:608-618.

565 Castaño-Miquel, L., and Lois, L.M. (2016). Kinetic analysis of plant SUMO conjugation
566   machinery. In: Plant Proteostasis: Methods and Protocols.--Lois, L.M., and
567   Matthiesen, R., eds.: Humana Press. 107-123.

568 Castaño-Miquel, L., Seguí, J., and Lois, L.M. (2011). Distinctive properties of Arabidopsis
569   SUMO paralogues support the in vivo predominant role of AtSUMO1/2 isoforms.
570   Biochem J 436:581-590.

571 Castaño-Miquel, L., Seguí, J., Manrique, S., Teixeira, I., Carretero-Paulet, L., Atencio, F., and
572   Lois, L.M. (2013). Diversification of SUMO-Activating Enzyme in Arabidopsis:
573   Implications in SUMO Conjugation. Molecular plant 6:1646-1660.

574 Castillo, A.G., Kong, L.J., Hanley-Bowdoin, L., and Bejarano, E.R. (2004). Interaction
575   between a geminivirus replication protein and the plant sumoylation system. J. Virol.
576   78:2758-2769.

577 Catala, R., Ouyang, J., Abreu, I.A., Hu, Y., Seo, H., Zhang, X., and Chua, N.H. (2007). The
578   Arabidopsis E3 SUMO ligase SIZ1 regulates plant growth and drought responses.
579   Plant Cell 19:2952-2966.

580 Conti, L., Nelis, S., Zhang, C.J., Woodcock, A., Swarup, R., Galbiati, M., Tonelli, C., Napier,
581   R., Hedden, P., Bennett, M., et al. (2014). Small Ubiquitin-like Modifier Protein
582   SUMO Enables Plants to Control Growth Independently of the Phytohormone
583   Gibberellin. Dev Cell 28:102-110.

584 Crooks, G.E., Hon, G., Chandonia, J.M., and Brenner, S.E. (2004). WebLogo: a sequence
585   logo generator. Genome Res 14:1188-1190.

586 Chosed, R., Tomchick, D.R., Brautigam, C.A., Mukherjee, S., Negi, V.S., Machius, M., and
587   Orth, K. (2007). Structural analysis of Xanthomonas XopD provides insights into
588   substrate specificity of ubiquitin-like protein proteases. J. Biol. Chem. 282:6773-6782.

589 Gareau, J.R., and Lima, C.D. (2010). The SUMO pathway: emerging mechanisms that shape
590   specificity, conjugation and recognition. Nat Rev Mol Cell Biol 11:861-871.

591 Glazebrook, J. (2005). Contrasting mechanisms of defense against biotrophic and
592   necrotrophic pathogens. Annu Rev Phytopathol 43:205 - 227.

593 Hotson, A., and Mudgett, M.B. (2004). Cysteine proteases in phytopathogenic bacteria:
594   identification of plant targets and activation of innate immunity. Curr Opin Plant Biol
595   7:384-390.

596 Huang, L., Yang, S., Zhang, S., Liu, M., Lai, J., Qi, Y., Shi, S., Wang, J., Wang, Y., Xie, Q.,
597   et al. (2009). The Arabidopsis SUMO E3 ligase AtMMS21, a homologue of
598   NSE2/MMS21, regulates cell proliferation in the root. The Plant Journal 60:666-678.

599 Ishida, T., Fujiwara, S., Miura, K., Stacey, N., Yoshimura, M., Schneider, K., Adachi, S.,
600   Minamisawa, K., Umeda, M., and Sugimoto, K. (2009). SUMO E3 Ligase HIGH
601   PLOIDY2 Regulates Endocycle Onset and Meristem Maintenance in Arabidopsis.
602   Plant Cell:1-14.

603 Jackson, A.L., and Linsley, P.S. (2010). Recognizing and avoiding siRNA off-target effects
604   for target identification and therapeutic application. Nat Rev Drug Discov 9:57-67.

605 Knipscheer, P., van Dijk, W.J., Olsen, J.V., Mann, M., and Sixma, T.K. (2007). Noncovalent
606   interaction between Ubc9 and SUMO promotes SUMO chain formation. EMBO J.
607   26:2797-2807.
608 Lee, I., and Schindelin, H. (2008). Structural insights into E1-catalyzed ubiquitin activation
609   and transfer to conjugating enzymes. Cell 134:268-278.
610 Lee, J., Nam, J., Park, H.C., Na, G., Miura, K., Jin, J.B., Yoo, C.Y., Baek, D., Kim, D.H.,
611   Jeong, J.C., et al. (2007). Salicylic acid-mediated innate immunity in Arabidopsis is
612   regulated by SIZ1 SUMO E3 ligase. Plant J. 49:79-90.
613 Lois, L.M. (2010). Diversity of the SUMOylation machinery in plants. Biochem Soc Trans
614   38:60-64.
615 Lois, L.M., and Lima, C.D. (2005). Structures of the SUMO E1 provide mechanistic insights
616   into SUMO activation and E2 recruitment to E1. EMBO J. 24:439-451.
617 Lois, L.M., Lima, C.D., and Chua, N.H. (2003). Small ubiquitin-like modifier modulates
618   abscisic acid signaling in Arabidopsis. Plant Cell 15:1347-1359.
619 Llorente, F., Alonso-Blanco, C., Sanchez-Rodriguez, C., Jorda, L., and Molina, A. (2005).
620   ERECTA receptor-like kinase and heterotrimeric G protein from Arabidopsis are
621   required for resistance to the necrotrophic fungus Plectosphaerella cucumerina. Plant J
622   43:165-180.
623 Mengiste, T. (2012). Plant Immunity to Necrotrophs. Annual Review of Phytopathology
624   50:267-294.
625 Miura, K., Lee, J., Jin, J.B., Yoo, C.Y., Miura, T., and Hasegawa, P.M. (2009). Sumoylation
626   of ABI5 by the Arabidopsis SUMO E3 ligase SIZ1 negatively regulates abscisic acid
627   signaling. Proc. Natl. Acad. Sci. U. S. A. 106:5418-5423.
628 Miura, K., Lee, J., Miura, T., and Hasegawa, P.M. (2010). SIZ1 controls cell growth and plant
629   development in Arabidopsis through salicylic acid. Plant Cell Physiol 51:103-113.
630 Miura, K., Okamoto, H., Okuma, E., Shiba, H., Kamada, H., Hasegawa, P.M., and Murata, Y.
631   (2013). SIZ1 deficiency causes reduced stomatal aperture and enhanced drought
632   tolerance via controlling salicylic acid-induced accumulation of reactive oxygen
633   species in Arabidopsis. The Plant Journal 73:91-104.
634 Miura, K., Rus, A., Sharkhuu, A., Yokoi, S., Karthikeyan, A.S., Raghothama, K.G., Baek, D.,
635   Koo, Y.D., Jin, J.B., Bressan, R.A., et al. (2005). The Arabidopsis SUMO E3 ligase
636   SIZ1 controls phosphate deficiency responses. Proc. Natl. Acad. Sc.i U. S. A.
637   102:7760-7765.
638 Miura, K., Sato, A., Ohta, M., and Furukawa, J. (2011). Increased tolerance to salt stress in
639   the phosphate-accumulating *Arabidopsis* mutants *siz1* and *pho2*. Planta 234:1191-
640   1199.
641 Murtas, G., Reeves, P.H., Fu, Y.F., Bancroft, I., Dean, C., and Coupland, G. (2003). A
642   nuclear protease required for flowering-time regulation in Arabidopsis reduces the
643   abundance of SMALL UBIQUITIN-RELATED MODIFIER conjugates. Plant Cell
644   15:2308-2319.
645 Naseem, M., Kaltdorf, M., and Dandekar, T. (2015). The nexus between growth and defence
646   signalling: auxin and cytokinin modulate plant immune response pathways. Journal of
647   experimental botany 66:4885-4896.
648 Nicholas, K.B., and Nicholas, H.B.J. (1997). GeneDoc: a tool for editing and annotating
649   multiple sequence alignments.
650 Rasband, W.S. (1997-2009). ImageJ, U. S. National Institutes of Health, Bethesda,
651 Maryland, USA, http://rsb.info.nih.gov/ij/.
652 Reiter, K., Mukhopadhyay, D., Zhang, H., Boucher, L.E., Kumar, N., Bosch, J., and Matunis,
653   M.J. (2013). Identification of Biochemically Distinct Properties of the Small

654   Ubiquitin-related Modifier (SUMO) Conjugation Pathway in Plasmodium falciparum.
655   Journal of Biological Chemistry 288:27724-27736.

656 Reiter, K.H., Ramachandran, A., Xia, X., Boucher, L.E., Bosch, J., and Matunis, M.J. (2015).
657   Characterization and Structural Insights into Selective E1-E2 Interactions in the
658   Human and Plasmodium falciparum SUMO Conjugation Systems. Journal of
659   Biological Chemistry.

660 Ribet, D., Hamon, M., Gouin, E., Nahori, M.A., Impens, F., Neyret-Kahn, H., Gevaert, K.,
661   Vandekerckhove, J., Dejean, A., and Cossart, P. (2010). Listeria monocytogenes
662   impairs SUMOylation for efficient infection. Nature 464:1192-1195.

663 Roden, J., Eardley, L., Hotson, A., Cao, Y., and Mudgett, M.B. (2004). Characterization of
664   the Xanthomonas AvrXv4 effector, a SUMO protease translocated into plant cells.
665   Mol .Plant. Microbe Interact. 17:633-643.

666 Saleh, A., Withers, J., Mohan, R., Marques, J., Gu, Y., Yan, S., Zavaliev, R., Nomoto, M.,
667   Tada, Y., and Dong, X. (2015). Posttranslational Modifications of the Master
668   Transcriptional Regulator NPR1 Enable Dynamic but Tight Control of Plant Immune
669   Responses. Cell host & microbe 18:169-182.

670 Sanchez-Duran, M.A., Dallas, M.B., Ascencio-Ibanez, J.T., Reyes, M.I., Arroyo-Mateos, M.,
671   Ruiz-Albert, J., Hanley-Bowdoin, L., and Bejarano, E.R. (2011). Interaction between
672   Geminivirus Replication Protein and the SUMO-Conjugating Enzyme Is Required for
673   Viral Infection. J Virol 85:9789-9800.

674 Saracco, S.A., Miller, M.J., Kurepa, J., and Vierstra, R.D. (2007). Genetic analysis of
675   SUMOylation in Arabidopsis: conjugation of SUMO1 and SUMO2 to nuclear proteins
676   is essential. Plant Physiol. 145:119-134.

677 Stulemeijer, I.J., and Joosten, M.H. (2008). Post-translational modification of host proteins in
678   pathogen-triggered defence signalling in plants. Molecular plant pathology 9:545-560.

679 Tomanov, K., Hardtke, C., Budhiraja, R., Hermkes, R., Coupland, G., and Bachmair, A.
680   (2013). SUMO Conjugating Enzyme with Active Site Mutation Acts as Dominant
681   Negative Inhibitor of SUMO Conjugation in Arabidopsis. J Integr Plant Biol.

682 van den Burg, H.A., Kini, R.K., Schuurink, R.C., and Takken, F.L. (2010). Arabidopsis small
683   ubiquitin-like modifier paralogs have distinct functions in development and defense.
684   Plant Cell 22:1998-2016.

685 Villajuana-Bonequi, M., Elrouby, N., Nordstrom, K., Griebel, T., Bachmair, A., and
686   Coupland, G. (2014). Elevated salicylic acid levels conferred by increased expression
687   of ISOCHORISMATE SYNTHASE 1 contribute to hyperaccumulation of SUMO1
688   conjugates in the Arabidopsis mutant early in short days 4. Plant J 79:206-219.

689 Walden, H., Podgorski, M.S., Huang, D.T., Miller, D.W., Howard, R.J., Minor, D.L., Jr.,
690   Holton, J.M., and Schulman, B.A. (2003). The structure of the APPBP1-UBA3-
691   NEDD8-ATP complex reveals the basis for selective ubiquitin-like protein activation
692   by an E1. Mol Cell 12:1427-1437.

693 Wang, H.D., Makeen, K., Yan, Y., Cao, Y., Sun, S.B., and Xu, G.H. (2011). OsSIZ1
694   Regulates the Vegetative Growth and Reproductive Development in Rice. Plant
695   Molecular Biology Reporter 29:411-417.

696 Wang, J., Hu, W., Cai, S., Lee, B., Song, J., and Chen, Y. (2007). The intrinsic affinity
697   between E2 and the Cys domain of E1 in ubiquitin-like modifications. Mol Cell
698   27:228-237.

699 Wang, J., Lee, B., Cai, S., Fukui, L., Hu, W., and Chen, Y. (2009). Conformational transition
700   associated with E1-E2 interaction in small ubiquitin-like modifications. J Biol Chem
701   284:20340-20348.

702 Wang, J., Taherbhoy, A.M., Hunt, H.W., Seyedin, S.N., Miller, D.W., Miller, D.J., Huang,
703   D.T., and Schulman, B.A. (2010). Crystal Structure of UBA2ufd-Ubc9: Insights into
704   E1-E2 Interactions in SUMO Pathways. PloS one 5:e15805.
705 Xu, P., Yuan, D., Liu, M., Li, C., Liu, Y., Zhang, S., Yao, N., and Yang, C. (2013).
706   AtMMS21, an SMC5/6 complex subunit, is involved in stem cell niche maintenance
707   and DNA damage responses in Arabidopsis roots. Plant Physiol.
708 Yoo, C.Y., Miura, K., Jin, J.B., Lee, J., Park, H.C., Salt, D.E., Yun, D.J., Bressan, R.A., and
709   Hasegawa, P.M. (2006). SIZ1 SUMO E3 ligase facilitates basal thermotolerance in
710   Arabidopsis independent of salicylic acid. Plant Physiol. 142:1548–1558.
711 Zinzalla, G. (2013). Understanding and exploiting protein?protein interactions as drug
712   targets. In: Understanding and Exploiting Protein?Protein Interactions as Drug
713   Targets: Future Science Ltd. 2-4.
714

715 FIGURE LEGENDS

716

732

Figure 1. Engineering SUMO activating enzyme large subunit, SAE2, for SUMOylation inhibition by blocking E1 (SAE2/SAE1) and E2 (SCE1) interactions.

(A) Schematic representation of protein-protein interactions during SUMO transfer from the E1 to the E2.

(B) SAE2^{UFDCt} domain (Ser436-Glu625) is essential for SUMO conjugation *in vitro*. SUMOylation assays were performed in the presence of Arabidopsis E1 (SAE2/SAE1a) or the deletion mutant E1ΔUFDCt (SAE2 ΔUFDCt/SAE1a), SUMO2, SCE1 and GST:CAT3Ct as substrate. Reactions in the absence of ATP were performed as negative control. Reaction mixtures were incubated at 37 ºC and stopped after 15 minute incubation. Reaction products were resolved by SDS-PAGE and examined by immunoblot analysis with anti-GST antibodies.

(C and D) SAE2^{UFDCt} inhibits SUMO conjugation *in vitro*. SUMOylation assays were performed at 37 ºC in the presence of E1, SUMO2, SCE1, GST:CAT3Ct as a substrate and in the absence or increasing amounts of SAE2^{UFDCt}. Reaction mixtures were stopped after 30 minutes and products were analyzed as in (B). Reactions were performed in quadruplicates and relative GST:CAT3Ct sumoylation quantified. Average values and SEM bars were plotted on the graph (D).

750

23

751
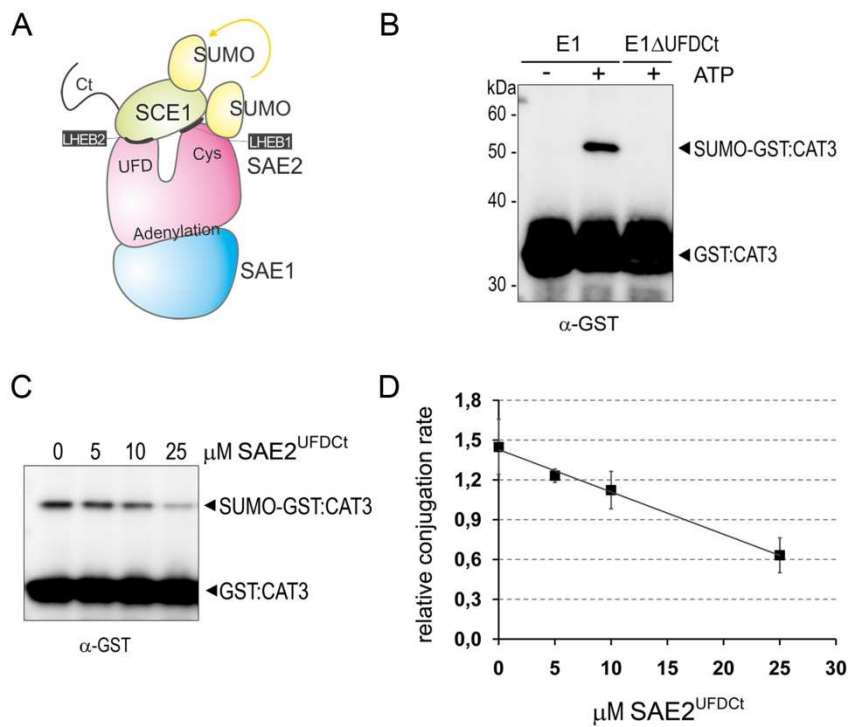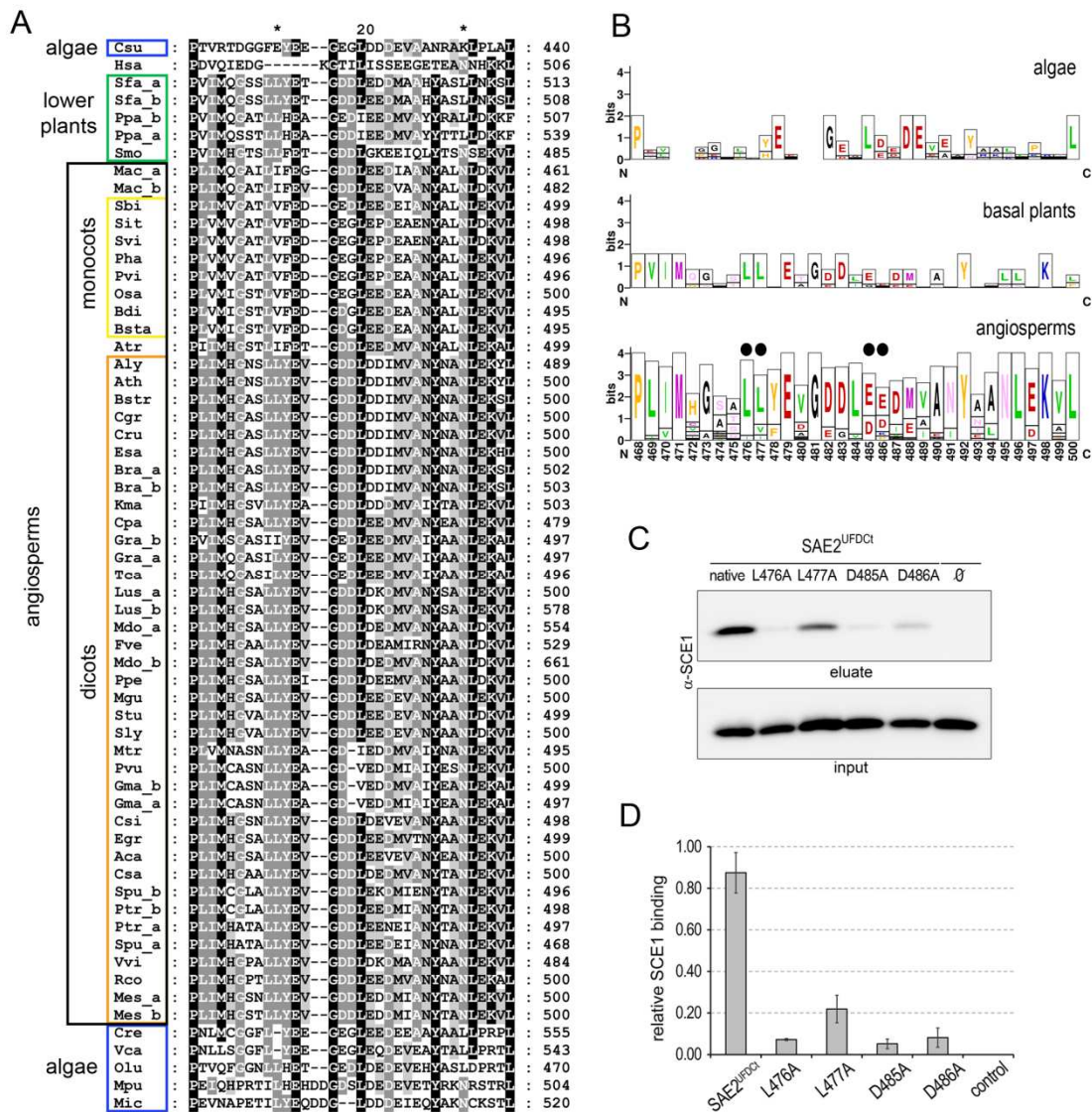
Figure 2. Molecular analysis of SAE2^{UFDCt}-SCE1 interactions.

(A) Viridiplantae (green algae and land plants) SAE2 LHEB2 sequence alignment. Sequence identity is indicated by black background and white letters (90%), gray background and white letters (70%) and light gray background and black letters (50%). Gaps in the alignment due to insertions or deletions are indicated by dashed lines. Residue numbers are shown to the right side of the sequences. Sequence names correspond to the first letter of the genus followed by the two first letters of the species (e.g. *A*rabidopsis *t*haliana, *Ath*). Sequences are listed in Supplemental table I.

(B) Graphical representation of plant LHEB2 consensus sequence determined from dicot and monocot SAE2^{UFDCt} sequence alignment. The overall height of the stack indicates the sequence conservation at that position, while the height of symbols within the stack indicates the relative frequency of each amino acid at that position. Amino acid predicted to have a role in SAE2^{UFDCt}-E2 interactions are indicated by black dots.

24

765   (C) *In vitro* polyHis pull-down assay of Arabidopsis SCE1 using His:SAE2UFDCt or its

766   mutant variants as a bait. Incubations in the absence of the bait were used as negative

767   controls (Ø).

768   (D) Aliquots of input and eluate fractions were resolved by SDS-PAGE and SCE1 levels were

769   analyzed by immunoblotting. Assays were performed in triplicates and relative SCE1 levels

770   quantified. Average values and standard error bars were plotted on the graph.

771

772
773
774
775
776
777
778
779
780
781
782
783
784
785
786
787
788
789
790
791
792
793
794
795
796
797
798
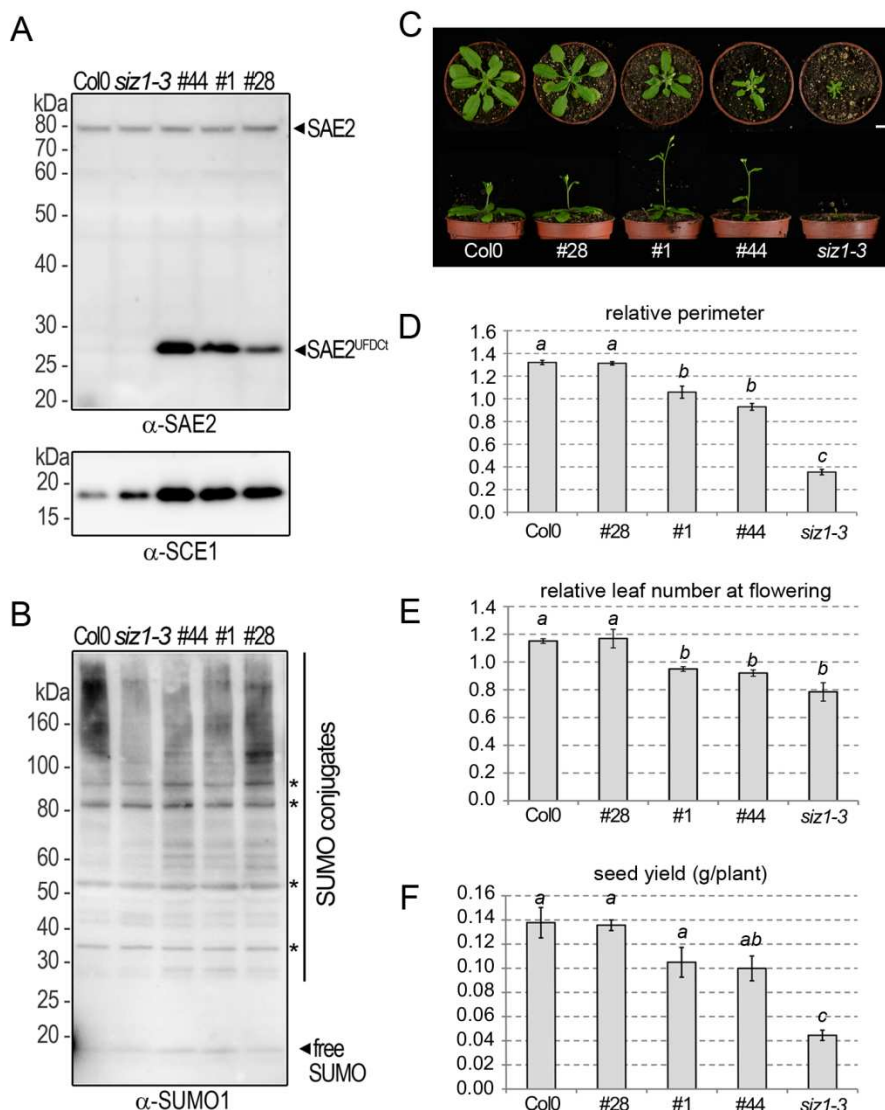
799 **Figure 3.** Effect of SAE2^{UFDCt} expression in endogenous SUMO conjugation and plant
800 development.

801 (A and B) Effect of SAE2^{UFDCt} expression in SUMO conjugates, SAE2 and SCE1 levels. Total
802 protein extracts from 4-day old seedlings were resolved by SDS-PAGE and examined by
803 immunoblot analysis with (A) anti-SAE2, anti-SCE1 and (B) anti-SUMO1 antibodies. Bands
804 that are not significantly reduced in SUMOylation deficient plants are indicated by asterisks.
805 (C) Developmental stage of 3-week old plants grown under long day conditions. Scale bar
806 represents 1 cm. Top and lateral views of representative plants are shown.

26

807 (D) Rosette perimeter according to ellipse perimeter defined by the three most external leaf

808 tips from each rosette. Average values and SEM from relative values obtained in four

809 biological replicates were plotted on the graph.

810 (E) Rosette leaf number at flowering was scored when the inflorescence had reached 1 cm.

811 Average values and SEM from relative values obtained in four biological replicates were

812 plotted on the graph.

813 (F) Seeds were harvested from individual fully dried plants and their weight measured.

814 Average values and SEM from relative values obtained in three biological replicates were

815 plotted on the graph.

816 *siz1-3* mutant was included as a control in all the analyses. T-test was performed and groups

817 with the same letter denote no statistical significant differences between them ($p > 0.05$).

818
819
820

A

831
832
833
834
835
836
837
838
839
840
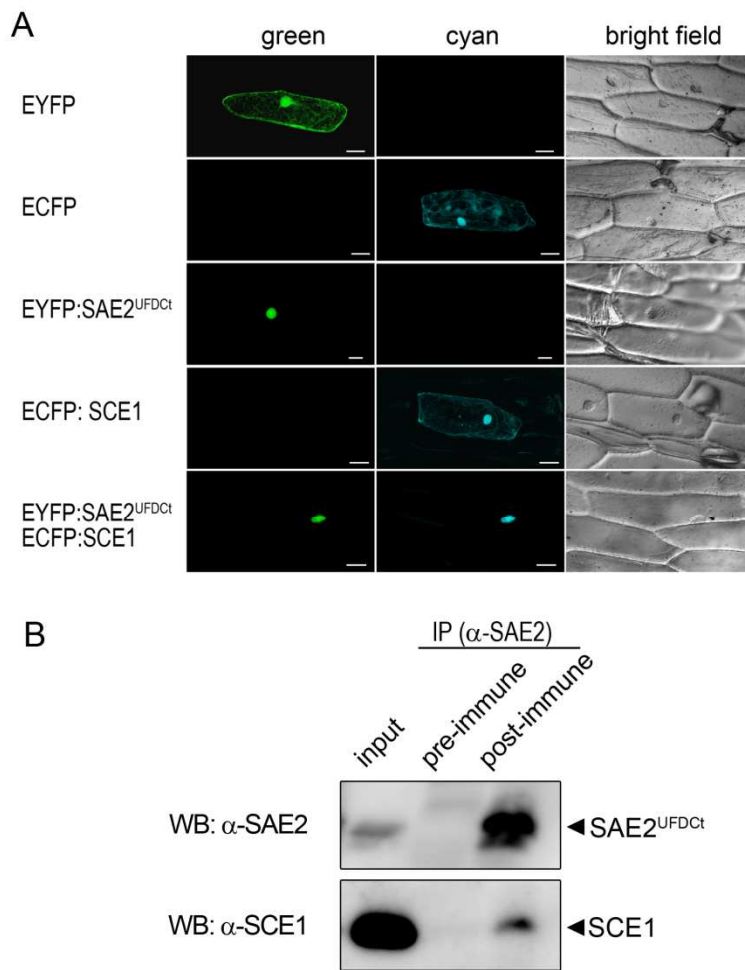
841 **Figure 4.** Analysis of SAE2^{UFDCt} SCE1 interactions *in vivo*.

842 (A) SAE2^{UFDCt} and SCE1 co-localize in the nucleus of onion cells. SAE2^{UFDCt} fused to EYFP

843 and SCE1 fused to ECFP were transiently expressed in onion epidermal cells, individually or

844 co-expressed. Cells expressing EYFP or ECFP were used as control. Light transmission

845 images of the fluorescent protein expressing cells are shown next to the corresponding

846 fluorescence image. Bars= 50 μm.

847 (B) Total protein extracts from Arabidopsis plants expressing the SAE2^{UFDCt} domain (line

848 #44) were subjected to immunoprecipitation with pre-immune serum or SAE2 post-

849 immunization serum. Input and immunoprecipitated protein fractions were analyzed by

850 immunoblotting using anti-SAE2 or anti-SCE1 antibodies.

851
852
853

28

854

855

856

857

858

859

860

861

862

863

864

865

866

867

868

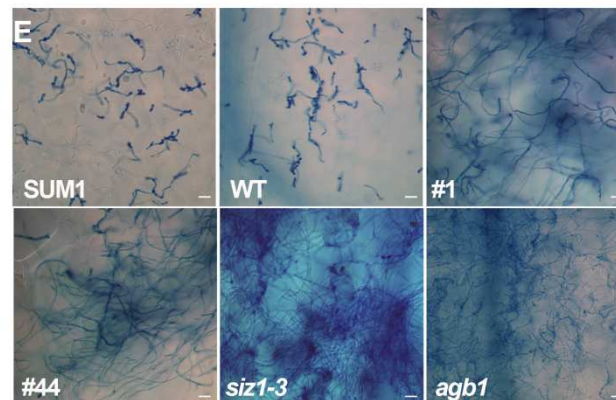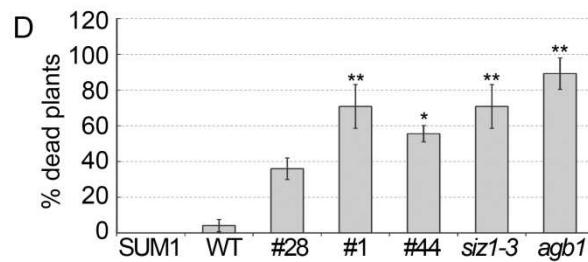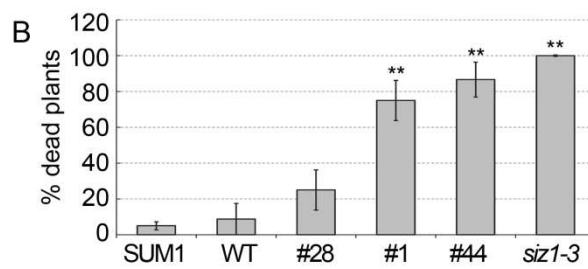869

870

871

872

873

874

875

876

877

878

879

880

881

882

883

884

885

886

887

888

889 **Figure 5.** Sumoylation is required for fungal resistance. Susceptibility of the indicated

890 Arabidopsis genotypes with altered SUMOylation activity to *Botrytis cinerea* (A-B) and

891 *Plectosphaerella cucumerina* (C-E) infection.

892 (A) Representative leaves detached from drop inoculated plants (10^6 spores/ml) with early

893 disease symptoms at 3 dpi (top). Phenotype of plants at 7 dpi that were inoculated on 4

894 leaves per plant (bottom).

895 (B) Percentage of dead plants at 15 dpi. Average values and SEM were calculated from 5

896 independent assays in which 8 plants per genotype were analyzed.

897 (C) Phenotypical appearance of representative plants at 7 days after spray inoculation with a

898 10^5 spores/ml suspension.

899 (D) Percentage of dead plans at 10 dpi. Average values and SEM were calculated from 3

900 independent assays in which 8 plants per genotype were analyzed.

901 (E) Trypan blue staining of *Plectosphaerella cucumerina* fungal hyphae growing on leaves at

902 3 dpi. Scale bar, 20 μm.

903 (F) Representative scheme of protein SUMOylation levels and fungal infection susceptibility.

904 Asterisks denote statistically significant differences with wild-type plants (Tukey test *$p<0.05$;

905 **$p<0.01$).

906

907

908
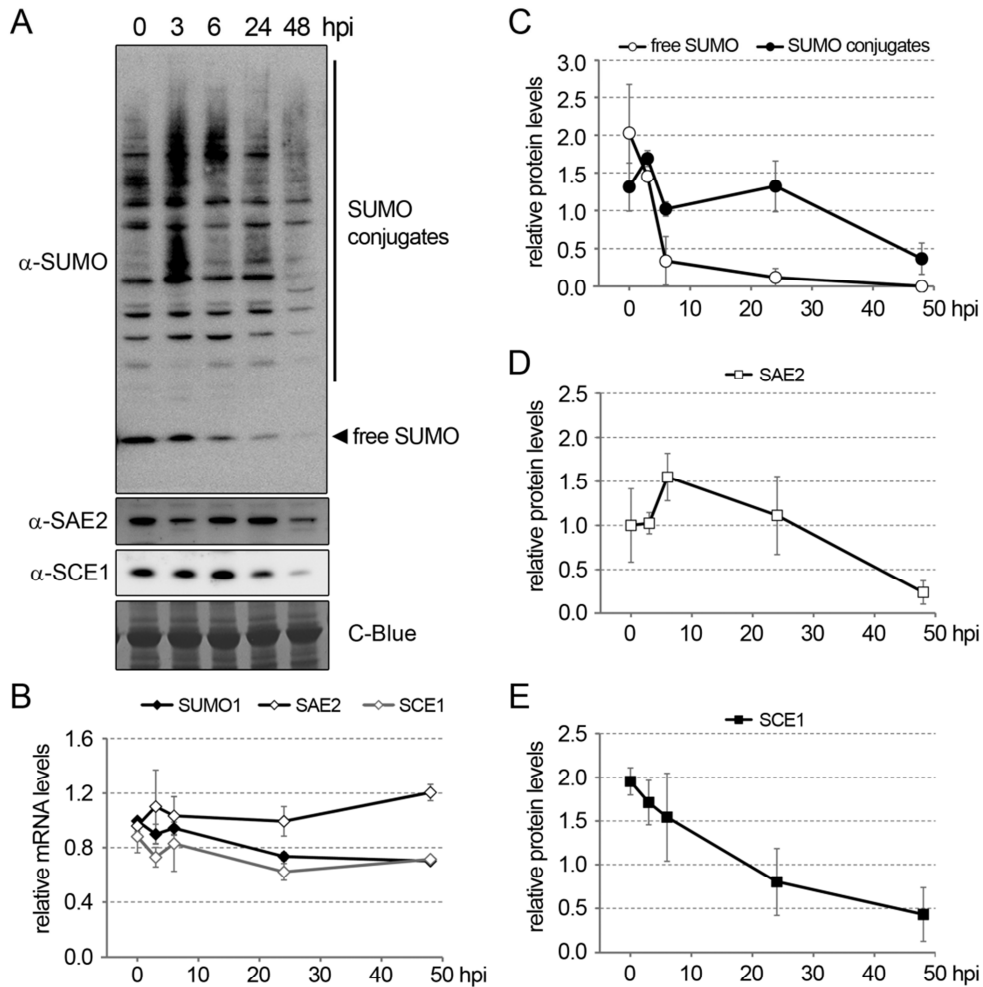
931

932 **Figure 6.** SUMO conjugates and SUMO conjugation machinery components SAE2 and
933 SCE1 protein levels diminish during fungal infection.

934 (A) Total protein extracts from 21-day old seedlings, before infection (0) or after 3, 6, 24 and
935 48 hpi (hours post-infection) were resolved by SDS-PAGE and examined by immunoblot
936 analysis with anti-SUMO1, anti-SAE2 and anti-SCE1 antibodies.

937 (B) mRNA levels corresponding to SUMO1, E1 activating enzyme large subunit (SAE2) and
938 E2 conjugating enzyme (SCE1) were quantified by qPCR. Collected data were normalized by
939 using AtUBC21 as a reference gene.

940 (C, D and E) Relative protein levels were quantified from the same biological samples as in
941 (B) and average values and SEM were plotted on the corresponding graphs. Quantifications
942 were performed from two or three- biological replicates.

31